JOURNAL OF CATALYSIS 100, 210–218 (1986)

CO Adsorption on (111) and (100) Surfaces of the Pt_3Ti Alloy: Evidence for Parallel Binding and Strong Activation of CO

S. P. MEHANDRU[1] AND ALFRED B. ANDERSON

Chemistry Department, Case Western Reserve University, Cleveland, Ohio 44106

AND

P. N. ROSS

Materials and Molecular Research Division, Lawrence Berkeley Laboratory, Berkeley, California 94720

Received July 6, 1985; revised February 25, 1986

An atom superposition and electron delocalization molecular orbital (ASED-MO) study has been made of CO adsorption on a 40-atom cluster model of the (111) surface and a 36-atom cluster model of the (100) surface of the Pt_3Ti alloy. Parallel binding to high-coordinate sites associated with Ti and low CO bond scission barriers are predicted for both surfaces. The preference for parallel adsorption is a consequence of the nature of the CO π-to-surface donation interactions. On Ti sites the π orbitals donate to the nearly empty Ti 3*d* band and the antibonding counterpart orbitals are empty. Thus the π donation makes substantial contributions to the adsorption bond order that are in addition to the contributions from 5σ donation and metal backbonding to the π^* orbitals. Altogether these bonding interactions favor the lying down orientation. On Pt sites, on the other hand, the π donation antibonding counterpart orbitals are occupied so that the net interaction with Pt is a closed-shell repulsion. CO bonds upright in order to minimize the π interaction and, concomitantly, the closed-shell repulsion, while maintaining 5σ donation and π^* backbonding stabilizations. Comparisons are made with the results for a 40-atom cluster model of the unalloyed Pt(111) surface. It is shown that the extended Hückel parameterization is inappropriate for studying CO adsorption to Pt with the ASED-MO theory because it incorrectly favors adsorption bonding through the oxygen end.

1. INTRODUCTION

The high heat of formation of the Pt_3Ti alloy (*1*) has been attributed to the strong interaction between the *d* orbitals of both metals (*2*). Understanding of this intermetallic bond has been the focus of a number of investigations in the recent past (*3–6*). These studies have examined modifications of the electronic and the chemisorptive properties of this alloy compared with the pure metals. Such modifications, often called "ligand effects," are considered to be the cause of the change in the catalytic activity of Pt_3Ti compared with the activity of the pure Pt metal.

The Pt_3Ti bulk structure is the fcc Cu_3Au-type structure as shown by X-ray diffraction analysis (*4*). Superlattice LEED patterns observed by Bardi and Ross (*5*) showed that the (111) and the (100) surfaces of Pt_3Ti are the simple terminations of the bulk structures in planes normal to the [111] and [100] directions, respectively. The {111} planes are all equivalent, consisting of alternating atomic rows of (50% Pt + 50% Ti) and 100% Pt as shown in Fig. 1. For the {100} planes, however, there are two possible inequivalent regular terminations when the crystal is cut normal to the [100] direction. These planes alternatively have (50% Pt + 50% Ti) and 100% Pt compositions (see Fig. 2). Bardi and Ross (*5*) have established that the clean annealed surface has the (50% Pt + 50% Ti) composition and not

---

[1] On leave from KM College, Delhi University, Delhi 110007, India.

0021-9517/86 $3.00

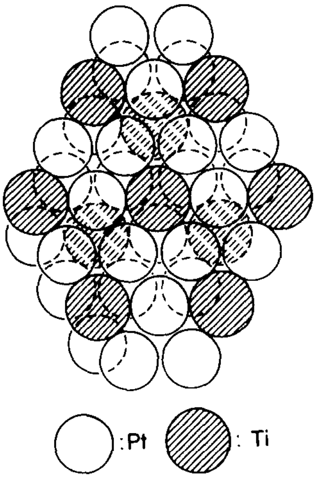

FIG. 1. $Pt_{30}Ti_{10}$ cluster model for the (111) surface of the Pt_3Ti alloy. The bulk lattice parameter of 3.906 Å was used in all the calculations.

the 100% Pt composition. Using dynamical LEED intensity analysis, they later determined that the (100) surface plane has a relaxed structure with the surface Pt atom plane lying ~0.5 Å above the surface Ti atom plane (*7*). Relaxation of the (111) surface has not yet been examined to our knowledge.

Bardi *et al.* (*4*) have studied the chemisorption of CO and H_2 on a polycrystalline Pt_3Ti alloy. They concluded from thermal desorption measurements that CO adsorbs with reduced binding energy to the alloy compared to pure platinum, and attributed this difference to the "ligand effect."

In this paper we have examined CO adsorption and dissociation on the (111) and the (100) surfaces of the alloy by using cluster models. We use the atom superposition and electron delocalization molecular orbital (ASED-MO) technique, the usefulness of which has been demonstrated in our previous CO adsorption studies on Pt (*8*) and Pd (*8b*) (111) and (100) surfaces, on potassium-promoted Pt(111) (*9*), and on Cr(110) surfaces (*10*), and the reader is referred to those works for further discussion of the ASED-MO theory. In those studies experimental valence state ionization potentials for oxygen 2*s* and 2*p* orbitals and for carbon 2*p* orbitals were used as the basis for parameterizing the theory. For the carbon 2*s* valence state ionization potential 20.0 eV was used in place of the experimental value of 16.59 eV. The value of 20.0 eV (*11*) is a small deviation from the extended Hückel value of 21.4 eV (*12*) and was used because it produced a better electronic structure for ethylene, as may be seen by comparing Refs. (*11*, *12*), and because of the historical importance of extended Hückel theory in its applications to hydrocarbon molecules. For almost all other atoms in ASED-MO studies, experimental valence state ionization potentials have been the basis for parameterization. It will be seen in this paper that for carbon the experimental 2*s* valence state ionization potential, 16.59 eV, is preferable over 20.0 eV and over the extended Hückel value, 21.4 eV. This is because bonding of CO to Pt through the oxygen end is slightly favored when 20.0 eV is used, a result of the 5σ orbital having an excessive oxygen 2*p* composition, as shown in Table 1. When the experimental value is used, binding through carbon is clearly and correctly favored. Other adsorption properties are not significantly affected by the change from 20.0 to 16.59 eV, though the gas phase CO bond energy calculation, shown in Table 1, is slightly improved. The parameters used in the present study are given in Table 2. Platinum, car-

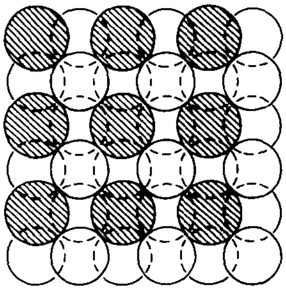

FIG. 2. $Pt_{27}Ti_9$ cluster model for the (100) surface of the alloy. The top layer has 50% Pt + 50% Ti, and the bottom layer has 100% Pt composition.

TABLE 1

Calculated Gas Phase CO Properties Based on Parameters in Table 2 but with Valence Atomic Orbital Ionization Potentials 1.5 eV Greater than Shown

Property	C 2*s*, IP = 20 eV			C 2*s*, IP = 16.59 eV			Expt
Bond length (Å)	1.11			1.11			1.128
Force constant (mdyn/Å)	19.77			19.78			18.99
Dissociation energy, D_e (eV)	9.54			10.96			11.36
Orbital	Charge on			Charge on			
	C	O	$-E$ (eV)	C	O	$-E$ (eV)	
5σ	1.03	0.97	12.52	1.28	0.72	12.32	—
π	0.66	1.34	15.15	0.66	1.34	15.19	—
4σ	1.06	0.94	17.83	0.87	1.13	16.35	—
3σ	0.63	1.37	32.29	0.51	1.48	31.27	—

Note. Experimental values are taken from K. P. Huber and G. Gerzberg, "Molecular Spectra and Molecular Structure. IV. Constants of Diatomic Molecules," Van Nostrand, New York, 1979. $-E$ are calculated molecular orbital energies. IP, ionization potential.

bon, and oxygen parameters are the same ones used in past studies of CO binding to Pt(111) surfaces (Refs. (*8, 9*)): valence state ionization potentials for carbon and oxygen are decreased 1.5 eV and those for platinum are increased by 1.5 eV to approximate self-consistency. The new adjusted carbon 2*s* valence state ionization potential is given in parentheses. Titanium parameters are the metallic ones.

The clusters used for modeling the single crystal alloy surfaces are assigned low spin. We use a bulk lattice parameter of 3.906 Å but the surface atoms are relaxed in 0.05-Å steps from their bulk positions, in a direction perpendicular to the surface plane, for the minimum energy. The CO bond length is optimized to the nearest 0.01 Å, the heights of CO above the surface and its lateral displacements are optimized to the nearest 0.05 Å, and the tilt of CO from the horizontal is optimized to the nearest 1 deg.

TABLE 2

Atomic Parameters Used in the Calculations: Principal Quantum Number (*n*), Ionization Potentials (IP) in eV, Slater Orbital Exponents (ξ), and Respective Coefficients (*C*) for Double-ξ *d* Functions[a]

Atom	*s*			*p*			*d*					
	n	IP	ξ	*n*	IP	ξ	*n*	IP	ξ_1	C_1	ξ_2	C_2
Pt	6	10.50	2.550	6	6.46	2.250	5	11.10	6.013	0.6562	2.396	0.5711
Ti	4	6.82	1.500	4	4.85	1.200	3	8.00	4.55	0.4206	1.400	0.7839
C	2	18.50 (15.09)	1.658	2	9.76	1.618						
O	2	26.98	2.146	2	12.12	2.127						

[a] Atomic parameters for Pt, C, and O are the same as used earlier in our previous CO adsorption studies on Pt(111) (*8, 9*). The ionization potentials for Ti are taken from W. Lotz, *J. Opt. Soc. Amer.* **60,** 206 (1970), and the Slater exponents are taken from J. W. Richardson, W. C. Nieuwpoort, R. R. Powell, and W. F. Edgell, *J. Chem. Phys.* **36,** 1057 (1962). The 4*s* and 4*p* exponents are determined as in our past studies of first row transition metals and the 4*p* ionization potential is determined from the lowest 4*s* → 4*p* excitation energy.

TABLE 3

Binding Site and Orientation, Binding Energy (BE), Bond Length (R_{CO}), Heights (h) of C and O above the Platinum Surface Plane, and Tilt Relative to the Surface Plane for CO Adsorbed on the Relaxed $Pt_{30}Ti_{10}$ Cluster Model of the (111) Surface[a]

Binding site	Orientation	BE (eV)	R_{CO} (Å)	h_C (Å)	h_O (Å)	Tilt (deg)
1-fold Pt	Perpendicular through C	1.54 (1.61)	1.16 (1.16)	2.00 (2.00)	3.16 (3.16)	—
	Perpendicular through O	1.52 (1.30)	1.16 (1.15)	2.91 (2.95)	1.75 (1.80)	—
1-fold Ti	Perpendicular through C	2.77 (2.41)	1.15 (1.15)	1.35[b] (1.35)	2.50 (2.50)	—
	Perpendicular through O	2.93 (2.46)	1.14 (1.14)	2.24 (2.29)	1.10[c] (1.15)	—
3-fold[d]	Perpendicular through C	1.66 (1.73)	1.21 (1.22)	1.50 (1.50)	2.71 (2.72)	—
	Perpendicular through O	Unstable				
Ti	Lying down[e] (C-end toward the 3-fold hollow)	2.87 (2.61)	1.18 (1.18)	1.25 (1.25)	1.11 (1.15)	7 (5)
	Lyding down[f] (C-end toward the 1-fold Pt)	2.67 (2.26)	1.16 (1.16)	1.60 (1.55)	1.11 (1.06)	25 (25)
Bridging Pt atoms	Parallel	0.89 (0.72)	1.18 (1.17)	1.95 (1.95)	1.95 (1.95)	0 (0)

[a] Numbers in parentheses are the results obtained by using the experimental IP for C 2*s*.

[b] The TiC distance is 1.90 Å.

[c] The TiO distance is 1.65 Å.

[d] This is the site between three Pt atoms having a Ti atom underneath in the second layer. The 3-fold site with a hole in the second layer is found to be less stable by 0.34 eV.

[e] See Fig. 3.

[f] See Fig. 3.

2. RESULTS AND DISCUSSION

2.1. *CO Adsorption on the (111) Surface*

We have used a two-layer-thick 40-atom cluster consisting of 30 Pt and 10 Ti atoms as shown in Fig. 1, for modeling the (111) surface of the Pt_3Ti alloy. The top layer has 16 Pt and 7 Ti atoms, and the bottom layer has 14 Pt and 3 Ti atoms. On relaxing only Ti atoms in the top layer, it is found that they move down 0.55 Å from their bulk positions. The binding site and the binding orientation of a single CO molecule are then studied on this relaxed surface. The calculated results are given in Table 3, and those obtained using the experimental carbon 2*s* valence state ionization potential are in parentheses. It is evident from the calculated binding energies that the binding of CO to the Ti sites is favored over its binding to the Pt sites. On the Ti sites, the binding energies for end-on orientation through either C or O and side-on orientation are very close. However, with the new carbon parameters the side-on orientation is most stable. That there is an oxygen–metal component to the chemisorption bond is indicated by the O 1*s* binding energies that are observed when CO adsorbs on the $Pt_3Ti(111)$ surface (*13*). CO also adsorbs side-on on Cr(110) according to electron energy loss vibrational analysis (*14a*) and electron stimulated ion desorption studies (*14b*), as well as an ASED-MO analysis (*10*).

In the most stable side-on orientation the O end of CO lies about 0.2 Å from the 1-fold Ti site and the C end orients toward the neighboring 3-fold hollow site. The CO axis is tilted 7 (5) deg relative to the surface plane (see Fig. 3). It is generally accepted that CO binds standing up through carbon on the 1-fold site of the Pt(111) surface. We have verified this by using a Pt_{40} cluster model (28 unpaired electrons) of the surface, as may be seen in Table 4. We find that the structure is nearly the same as on

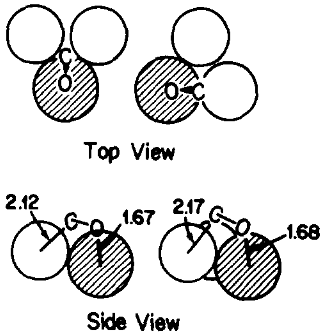

FIG. 3. The lying-down orientations of CO on the Ti site of the 40-atom alloy cluster model of Fig. 1.

the 1-fold Pt site of the alloy, but the CO adsorption energy on the alloy Pt sites is less than that on the unalloyed Pt surface. On the $Pt_{30}Ti_{10}$ cluster, the binding energy of CO in the perpendicular orientation on the 3-fold site having a Ti atom underneath in the second layer is calculated to be 0.12 (0.12) eV greater than the same orientation on the 1-fold site. But it is still 0.13 (0.20) eV less stable than the 1-fold site of the $Pt_{40}(111)$ cluster. This decrease in the binding energy of CO on the surface Pt atoms of the alloy compared to pure Pt, as well as the change in the site preference from the 1-fold atop to the high-coordinate site, is due to the ligand effects in the alloy. It may, however, be noted that the reduction in CO binding energy on the alloy surface would occur only if the Ti sites are blocked. In fact, this was observed experimentally: initially adsorbed CO leads to the blocking of the Ti sites by oxygen ions formed from its dissociation and the carbon appears to go into the bulk (*13*). Subsequently, CO will adsorb only on the Pt sites with a presumably weakened adsorption energy.

The energy level correlation diagram for CO adsorbed on the Ti atom in the lying-down orientation with the carbon end toward the 3-fold hollow surface site is shown in Fig. 4. It may be seen that CO binds to the surface by means of 5σ and π donation bonds to the filled Pt + Ti band region. The antibonding counterparts are high lying and empty, so the donation results in a small positive charge of 0.17 on CO. Overall, there are three donation bonds to the surface and two back-donation bonds from the metal to the π^* orbitals of CO. These orbital stabilizations are all stronger than they are for the upright orientation where the orbital overlaps with the surface orbitals are reduced because only the carbon atom is involved. CO binds parallel to the Cr(110) surface according to experimental analysis (*14*) and the reason is the same as above, as we have recently shown (*10*). When more *d* electrons are present in the transition metal, the situation may change. Platinum has a nearly filled *d* band and since the antibonding counterpart orbitals to the π dona-

TABLE 4

Binding Site and Orientation, Binding Energy (BE), Bond Length (R_{CO}), and Heights (h) of C and O above the Relaxed Surface Plane for CO Adsorbed on the Pt_{40} Cluster of (111) Surface[a]

Binding site	Orientation	BE (eV)	R_{CO} (Å)	h_C (Å)	h_O (Å)
1-fold	Perpendicular through C	1.79 (1.93)	1.16 (1.16)	2.05 (2.05)	3.21 (3.21)
	Perpendicular through O	1.83 (1.64)	1.16 (1.15)	2.95 (2.95)	1.80 (1.80)
2-fold	Perpendicular through C	1.65 (1.77)	1.18 (1.18)	1.65 (1.65)	2.83 (2.83)
	Perpendicular through O	0.89 (0.65)	1.16 (1.16)	2.61 (2.61)	1.45 (1.45)
3-fold	Perpendicular through C	1.66 (1.79)	1.19 (1.19)	1.55 (1.55)	2.74 (2.74)
	Perpendicular through O	0.50 (0.24)	1.16 (1.16)	2.51 (2.51)	1.35 (1.35)

[a] Numbers in parentheses are the results obtained by using the experimental IP for C 2*s*. The relaxation consists of a 0.05-Å decrease in separation between the two Pt planes.

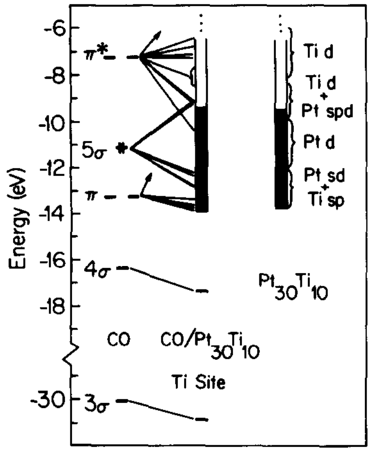

FIG. 4. Energy level correlation diagram for CO adsorbed in the lying-down orientation on the Ti site of the $Pt_{30}Ti_{10}$ cluster model of the (111) surface. The C-end orients toward the 3-fold hollow surface site. The correlation lines are drawn for orbitals having 0.04 or more electrons on CO.

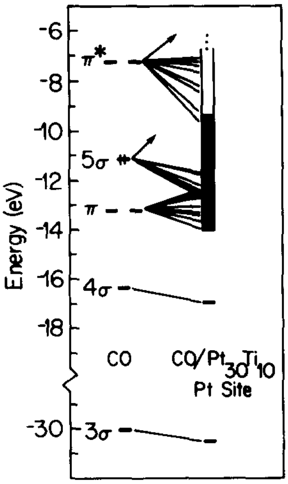

FIG. 5. Same as in Fig. 4 for CO in the side-on orientation bridging two Pt atoms on the (111) surface of the alloy.

tion orbitals are doubly occupied, the resulting closed-shell repulsion causes CO to stand upright with the resulting bonding to the surface consisting in a strong 5σ donation and weak back-donations to the π* orbitals with a resulting small positive net charge on CO (*8*). In this case, cathodic shifting of the *d* band causes CO to move from the 1-fold site to 2- and 3-fold sites where the back-donation to the π* orbitals is enhanced and substantial charge is transferred to CO (*9*).

It is easily understood why parallel binding of CO over two Pt atoms on the (111) surface of the alloy is very weak. In this case, as shown in Fig. 5, the antibonding counterparts to the donation bonds lie in the filled platinum band region and the resulting closed-shell repulsion causes CO to stand upright.

The tilted side-on bonding configuration with the carbon end toward the 3-fold hollow site may be considered as a precursor state for the dissociation of CO on this surface. When stretched by 0.55 (0.60) Å on this site, it reaches its transition state with an activation barrier of 0.74 (1.26) eV, showing strong activation consistent with the experimental observation of dissociation at near-ambient temperature (*13*). Figure 6 shows the orbital stabilizations for CO in its transition state. As the CO bond is stretched, the π* orbitals shift down, thus increasing the interaction with the filled Pt

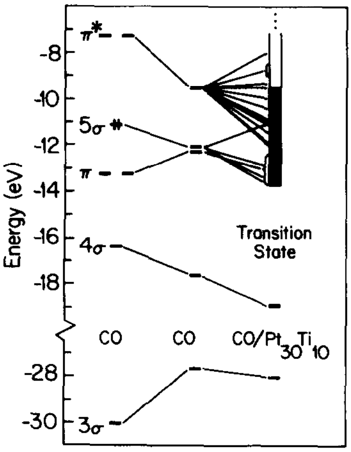

FIG. 6. Same as in Fig. 4 for CO in the transition state on the (111) surface of the alloy. The second column shows the energy levels of CO having the transition state structure but without the cluster.

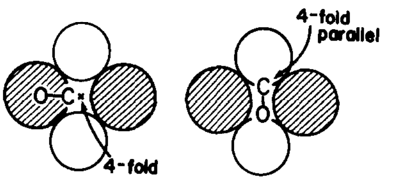

FIG. 7. Some of the adsorption sites studied on the cluster model of Fig. 2. The cross symbol (×) represents perpendicular orientation on this site.

+ Ti *d* bands. This gives rise to increased charge transfer to the π^* orbitals.

2.2. *CO Adsorption on the (100) Surface*

We model the (100) surface of the Pt_3Ti alloy by employing a 36-atom cluster (Fig. 2). The top layer contains 9 Ti and 9 Pt atoms and represents the (50% Pt + 50% Ti) truncation as discussed in the Introduction. The bottom layer has 18 Pt atoms and models the 100% Pt truncation. On relaxing the top layer atoms, it is found that the Ti atoms move down by 0.65 Å and the Pt atoms move up by 0.05 Å from their bulk positions. The calculated relative displacement of the Pt and the Ti atoms on the surface plane (0.7 Å) is quite close to the value of ~0.5 Å estimated by Ross and co-workers using dynamical LEED intensity analysis (*7*). The adsorption of CO is then studied on this relaxed surface. Figure 7 shows some of the binding sites and the binding orientations studied on the 36-atom cluster model. The calculated results are presented in Table 5. The binding of CO on the Ti site in the side-on configuration is distinctly favored over the other sites and orientations. In this orientation the oxygen end of the CO molecule lies 0.29 (0.27) Å from the top of the Ti atom and the carbon end lies 0.45 (0.47) Å toward the Ti site from the center of the neighboring 4-fold hollow site. The next site in terms of the decreasing binding energy is the 4-fold hollow site on which the carbon and the oxygen ends of CO point toward the surface Pt atoms. The CO orbital stabilizations on the most stable lying-down configuration are similar to those shown in Fig. 4 for the (111) surface.

We have also calculated the CO bond scission barrier for CO adsorbed on the most stable site on the (100) surface. When the CO bond is stretched by 0.55 (0.60) Å from its equilibrium value it reaches its transition state with a barrier of 0.91 (1.30)

TABLE 5

Binding Site and Orientation, Binding Energy (BE), Bond Length (R_{CO}), Heights (*h*) of C and O above the Platinum Surface Plane for CO Adsorbed on the Relaxed $Pt_{27}Ti_9$ Cluster Model of the (100) Surface[a]

Binding site	Orientation	BE (eV)	R_{CO} (Å)	h_C (Å)	h_O (Å)
1-fold Pt	Perpendicular through C	2.72 (2.77)	1.17 (1.17)	2.00 (2.00)	3.17 (3.17)
	Perpendicular through O	2.57 (2.35)	1.16 (1.16)	2.91 (2.91)	1.75 (1.75)
1-fold Ti	Perpendicular through C	2.96 (2.60)	1.15 (1.15)	1.20[b] (1.20)	2.35 (2.35)
	Perpendicular through O	3.05 (2.60)	1.14 (1.15)	2.09 (2.10)	0.95[c] (0.95)
4-fold	Perpendicular through C	2.99 (2.78)	1.21 (1.21)	1.05 (1.05)	2.26 (2.26)
	Perpendicular through O	1.52 (1.14)	1.15 (1.15)	2.05 (2.05)	0.90 (0.90)
Ti	Parallel[d]	3.93 (3.53)	1.21 (1.21)	0.90 (0.90)	0.90 (0.90)
4-fold	Parallel[e]	3.71 (3.38)	1.16 (1.16)	1.50 (1.45)	1.50 (1.45)

[a] Numbers in parentheses are the results obtained by using the experimental IP for C 2*s*.

[b] The TiC distance is 1.90 Å.

[c] The TiO distance is 1.65 Å.

[d] In this orientation the C end lies 0.47 Å toward the Ti atom from the 4-fold site.

[e] See Fig. 7.

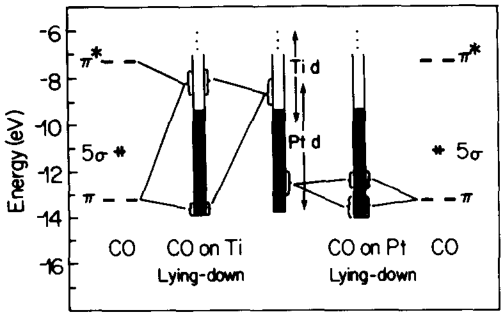

FIG. 8. Qualitative correlation diagram for CO in the lying-down orientation on the Ti and the Pt sites, on the (111) surface.

eV which is similar to that calculated for the (111) surface.

3. SUMMARY

We have made a theoretical study of CO adsorption on the (111) and (100) surfaces of the Pt_3Ti alloy. On the clean surfaces, binding of CO on the Ti sites is favored compared to the binding on the Pt sites. On the (111) surface side-on bonded CO with the carbon end oriented toward the 3-fold hollow surface site is most stable. In the lying-down orientation, bonding to the surface is a result of the 5σ and π donation interactions; the antibonding counterparts of both are high-lying and empty. The antibonding counterparts of the π donation orbitals are occupied when CO lies down on the Pt sites and this causes a closed-shell repulsion which is reduced only when CO bonds upright by the familiar 5σ and π^* interactions. A qualitative understanding of this difference in stability for CO binding on the Ti and the Pt sites in the lying-down configuration is given in Fig. 8. When CO bonds on the Ti sites, the π orbitals mix with empty Ti *d* band orbitals. The antibonding counterpart orbitals are therefore also empty so that the π donation contributes substantially to the chemisorption bond order. This is shown on the left side of Fig. 8. When CO bonds parallel on the Pt sites, the CO π orbitals interact with the lower-lying filled Pt *d* band region and therefore their antibonding counterparts lie within the filled Pt + Ti *d* band. The net π interaction with the surface becomes a closed-shell repulsion. This is shown on the right side of Fig. 8. The same explanation holds true for the favored lying-down configuration of CO on the (100) surface of the alloy.

We calculate small CO bond scission barriers on the (111) and the (100) alloy surfaces, which shows considerable bond activation of the lying-down CO molecules. Finally, we have shown that the use of the experimental carbon 2*s* valence ionization potential instead of the traditional extended Hückel value is necessary for the prediction that CO binds to platinum through the carbon end instead of through the oxygen end. The orientation preference depends on the polarization of the 5σ orbital. The proper carbon 2*s* ionization potential has this orbital polarized toward carbon so that CO forms a stronger 5σ donation to platinum through the carbon end. Other results are not qualitatively altered by using the new carbon 2*s* value.

ACKNOWLEDGMENTS

This study was supported by NASA Grant NAG-3-341 from the Lewis Research Center, Cleveland, Ohio. P.N.R. acknowledges support by the Assistant Secretary for Fossil Energy, Office of Coal Utilization, Advanced Energy Conversion Systems Division of the U.S. Department of Energy under Contract DE-AC03-76SF00098.

REFERENCES

1. (*a*) Meschter, P. J., and Worrell, W. L., *Met. Trans.* **7A**, 299 (1976). (*b*) Brewer, L., and Wengert, P. R., *Met. Trans.* **4**, 83 (1973).
2. Brewer, L., *in* "Phase Stability in Metals and Alloys" (P. Rudman, J. Stringer, and R. I. Jaffee, Eds.), p. 39. McGraw-Hill, New York, 1967.
3. Derry, G. N., and Ross, P. N., *Solid State Commun.* **52**, 151 (1984).
4. Bardi, U., Somorjai, G. A., and Ross, P. N., *J. Catal.* **85**, 272 (1984).
5. Bardi, U., and Ross, P. N., *Surf. Sci.* **146**, L555 (1984).
6. Bardi, U., and Ross, P. N., *J. Vac. Sci. Technol. A* **2**, 1461 (1984).

7. Bardi, U., Maglietta, M., Torrini, M., Zanazzi, E., and Ross, P. N., presented at the First International Conference on the Structure of Surfaces, Berkeley, Calif., Aug. 13–16, 1984.
8. (*a*) Ray, N. K., and Anderson, A. B., *Surf. Sci.* **119,** 35 (1982). (*b*) Anderson, A. B., and Awad, Md. K., *J. Amer. Chem. Soc.* **107,** 7854 (1985).
9. Ray, N. K., and Anderson, A. B., *Surf. Sci.* **125,** 803 (1983).
10. Mehandru, S. P., and Anderson, A. B., *Surf. Sci.*, in press.
11. Anderson, A. B., *J. Chem. Phys.* **65,** 1729 (1976).
12. Anderson, A. B., *J. Chem. Phys.* **61,** 4545 (1974).
13. Bardi, U., Dahlgren, D., and Ross, P. N., Lawrence Berkeley Laboratory Report LBL-20004, in press.
14. (*a*) Shinn, N. D., and Madey, T. E., *Phys. Rev. Lett.* **53,** 2481 (1984). (*b*) Shinn, N. D. and Madey, T. E., *J. Chem. Phys.* **83,** 5928 (1985).